

Magnetostriction and anisotropy compensation in $Tb_xDy_{0.9-x}Nd_{0.1}Fe_{1.93}$ [$0.2 \leq x \leq 0.4$]

S Narayana Jammalamadaka,^{1,a)} G. Markandeyulu,^{1,b)} and Krishnan Balasubramaniam²

¹Department of Physics, Advanced Magnetic Materials Laboratory, Indian Institute of Technology Madras, Chennai 600036, India

²Department of Mechanical Engineering, Centre for Non Destructive Evaluation, Indian Institute of Technology Madras, Chennai 600036, India

(Received 6 October 2010; accepted 6 November 2010; published online 13 December 2010)

Structure and magnetostriction of $Tb_xDy_{0.9-x}Nd_{0.1}Fe_{1.93}$ ($0.2 \leq x \leq 0.4$) compounds are investigated. All the compounds are found to stabilize in MgCu₂-type C15 cubic Laves phase structure. The easy magnetization direction changes from $\langle 100 \rangle$ ($x=0.2$) to $\langle 111 \rangle$ ($x=0.3$) through an intermediate state at $x=0.25$. Anisotropy compensation is realized near $x=0.25$ for the $Tb_xDy_{0.9-x}Nd_{0.1}Fe_{1.93}$ compounds. The Laves phase compound $Tb_{0.4}Dy_{0.5}Nd_{0.1}Fe_{1.93}$ has large spontaneous magnetostriction (1670×10^{-6}) and a low anisotropy at room temperature which could make it a good candidate material for magnetostriction applications. © 2010 American Institute of Physics. [doi:10.1063/1.3525577]

The binary C15 cubic Laves phase RFe_2 (R = rare-earth elements) compounds are known to exhibit giant magnetostriction values and large magnetocrystalline anisotropy at room temperature.¹⁻³ Giant magnetostriction has been reported at room temperature in binary compounds $TbFe_2$ (2630×10^{-6} at 25 kOe) and $DyFe_2$ (1610×10^{-6} at 25 kOe) with a cubic Laves structure.^{4,5} For the purpose of applications, many studies have focused on the anisotropy compensation of these systems in the past three decades, such as $Tb_xDy_{1-x}Fe_2$ and $Tb_xHo_{1-x}Fe_2$.⁶⁻⁹ Binary rare earth compounds have one degree of freedom, viz., x , which permits only the minimization of the first order (largest) anisotropy constant K_1 . By adding a third rare earth element, an additional degree of freedom is obtained and both the first and the second order anisotropy constants K_1 and K_2 can be minimized.¹⁰

According to single ion model, proposed by Clark *et al.*,¹ the spontaneous magnetostriction (λ_{111}) values of $NdFe_2$ and $PrFe_2$ are 2000×10^{-6} and 5600×10^{-6} , respectively, at 0 K. $NdFe_2$ has the easy magnetization direction (EMD) along $\langle 100 \rangle$ at room temperature.¹¹ The anisotropy of $NdFe_2$ and $PrFe_2$ is unknown as these materials could not be prepared so far with a single phase, by normal methods. Several reports have shown the anisotropy compensation of the compound $Tb_xDy_{1-x}Fe_2$, with Pr as third element to minimize the K_1 and K_2 .^{7,9} However, very little work has been carried to compensate the anisotropy with the element Nd even though the λ_{111} of this material is very high.¹ Shi *et al.*¹² reported the anisotropy compensation and magnetostriction studies on high pressure synthesized $Tb_xNd_{1-x}Fe_{1.9}$. Based on our preliminary magnetization and magnetostriction results, at $x=0.1$ minimum anisotropy is observed in the compound $Tb_{0.3}Dy_{0.7-x}Nd_xFe_{1.93}$ ($0 \leq x \leq 0.2$). Hence, we chose Nd composition as 0.1 in the present study. In this letter we report the results on structure, magnetostriction, and anisotropy compensation of $Tb_xDy_{0.9-x}Nd_{0.1}Fe_{1.93}$ ($0.2 \leq x \leq 0.4$)

compounds which were prepared using arc melting technique.

All the compounds were prepared by arc melting the constituent elements (rare earths of 99.9% purity and Fe of 99.95%) employing in an arc furnace (Centorr Associates, USA). The constituent elements were weighed in stoichiometric proportions and were melted together under argon atmosphere. The melting was carried out several times to ensure homogenous mixing of the elements. The weight loss after the final melting was less than 0.5%. The arc-melted ingots were sealed in quartz tubes under a pressure of $\sim 10^{-6}$ torr and homogenized at 900 °C for a week and were then furnace cooled. The compounds were characterized for the structural aspects by powder XRD (using Panalytical x-ray diffractometer) and employing $Cu K\alpha$ radiation. The reflections were indexed according to the allowed reflections for the C15-type Laves phase structure. We could obtain very good Rietveld fitting of the x-ray diffraction pattern by assuming the occupation of Nd at respective sites. Magnetostriction measurements were carried out using the strain gauge technique at 300 K. In order to find the EMD, the XRD on the magnetically oriented samples were taken. For this purpose powder particles were mixed with epoxy and were then aligned in the presence of magnetic field at 20 kOe with field perpendicular to the substrate. The epoxy was allowed to cure while the field was present.

Figure 1 shows the powder XRD patterns of $Tb_xDy_{0.9-x}Nd_{0.1}Fe_{1.93}$ ($x=0.2, 0.25, 0.3, 0.35, \text{ and } 0.4$). The compounds are formed in single phase with the cubic Laves phase and are confirmed by Rietveld refinement. The magnetization at room temperature for the $Tb_xDy_{0.9-x}Nd_{0.1}Fe_{1.93}$ is shown in Fig. 2(a). It is evident that for all the compounds, the magnetization values are not saturated up to 12 kOe. With the magnetic field, magnetization increases as though it would saturate at higher fields. Figure 2(b) shows the curves of M/M_{\max} versus H , where M_{\max} denotes the magnetization of compounds at 12 kOe. It is evident from Fig. 2(b) that the magnetization of $Tb_{0.25}Dy_{0.65}Nd_{0.1}Fe_{1.93}$ is most easily saturated among all the samples, indicating low magnetic anisotropy due to anisotropy compensation near that composition.

^{a)}Electronic mail: surya.jammalamadaka@fys.kuleuven.be.

^{b)}Author to whom correspondence should be addressed. Electronic mail: mark@physics.iitm.ac.in.

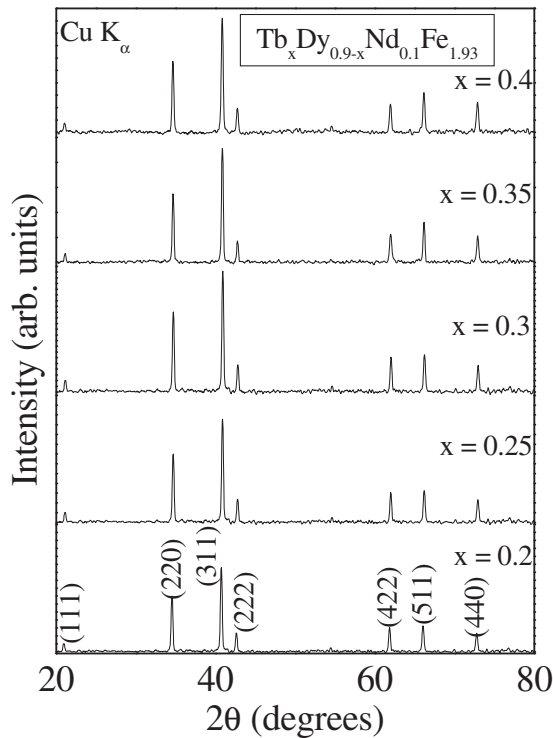


FIG. 1. Powder XRD patterns of $Tb_xDy_{0.9-x}Nd_{0.1}Fe_{1.93}$ compounds.

The saturation magnetization (M_S) is obtained from Honda plots (M versus $1/H$). The variation of M_S is shown as an inset in Fig. 2(b). The M_S increases with Tb concentration from 56 emu/g (at $x=0.2$) to 64 emu/g (at $x=0.4$). The increase is due to the larger effective moment of Tb^{3+} ($10.50 \mu_B$) compared to that of Dy^{3+} ($7.08 \mu_B$). In addition,

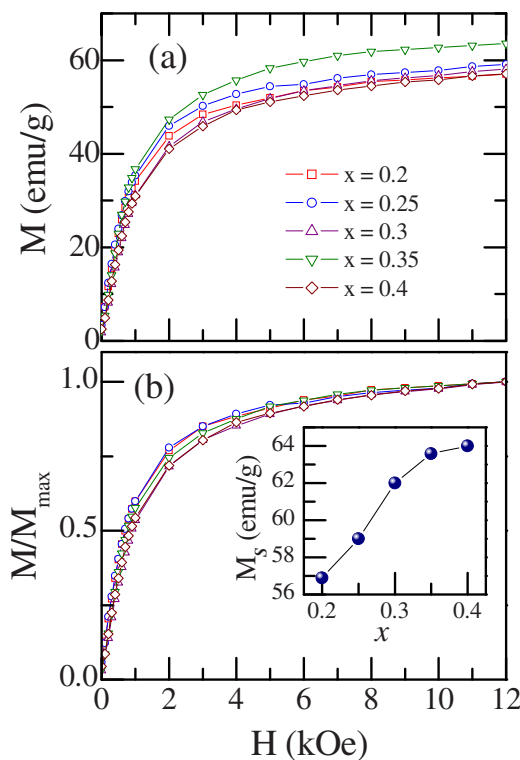


FIG. 2. (Color online) (a) Variation of magnetization with the applied magnetic field (b) M/M_{max} vs H curves, concentration dependence of saturation magnetization M_S at room temperature is shown as an inset.

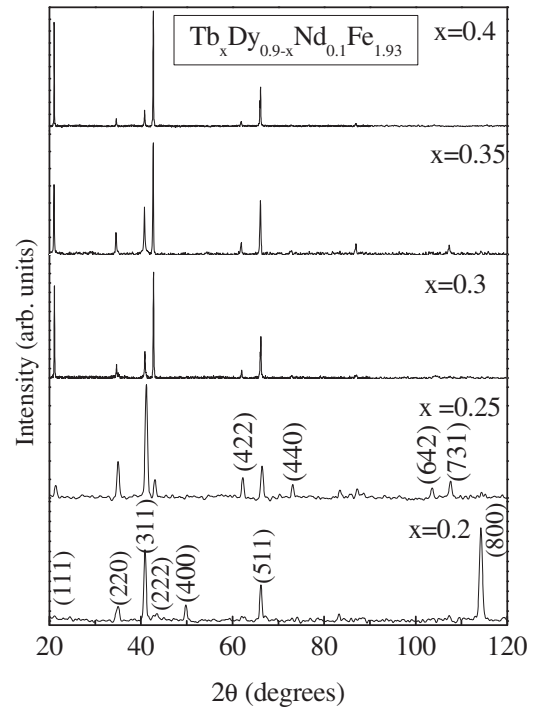


FIG. 3. XRD patterns for magnetically aligned $Tb_xDy_{0.9-x}Nd_{0.1}Fe_{1.93}$ particles at room temperature.

tion, the ferromagnetic ordering between the Tb (heavy rare earth) sublattice and the Dy (heavy rare earth) sublattice could also be a reason for the increase in the M_S .

The XRD patterns at room temperature for the magnetically aligned powders of $Tb_xDy_{0.9-x}Nd_{0.1}Fe_{1.93}$ compounds are represented in Fig. 3. The (800) peak is the intense reflection for the $x=0.2$, which indicates that the EMD aligns along $\langle 100 \rangle$ directions in accordance with the EMD of Dy and Nd is along $\langle 100 \rangle$.¹ For the composition $x=0.2$, the (311) peak intensity is 75% of the (800) peak intensity. At this juncture it is worth mentioning that in $Tb_{0.2}Dy_{0.54}Pr_{0.26}(Fe_{0.9}B_{0.1})$, minimum anisotropy is reported at room temperature (RT) and it is evidenced by comparing the XRD peak intensities of (311) and (800) reflections in magnetically aligned samples.⁷ Hence, we anticipate that in our case the anisotropy compensation is possible in the range between $0.2 \leq x \leq 0.25$. EMD changed from $\langle 100 \rangle$ (at $x=0.2$) to $\langle 111 \rangle$ (at $x=0.3$) through an intermediate state at $x=0.25$. At $x=0.25$, the most intense peak is (311). It can be said that the EMD for $x=0.25$ compound is along $\langle 113 \rangle$ which is a nonmajor axis. In pseudobinary RFe_2 compounds, at low temperatures, nonmajor axes of easy magnetization were observed and this phenomenon was explained by taking into account the action of the anisotropy constant K_3 , as K_1 and K_2 of these compounds are small due to the compensation around spin reorientation temperature (SRT).¹³ The intensity of (800) and (400) peaks weakens, while that of (111) peaks strengthens with increasing the Tb content (≥ 0.3), which indicates that the EMD is along $\langle 111 \rangle$. It can be summarized that the EMD at room temperature of these alloys rotates continuously from $\langle 100 \rangle$ for $x=0.2$ to $\langle 111 \rangle$ for $x=0.40$ through an intermediate direction $\langle 113 \rangle$ for $x=0.25$ due to the anisotropy compensation.

Spontaneous magnetostriction (λ_{111}) leads to distortion of the crystal structure when a magnetic material is cooled

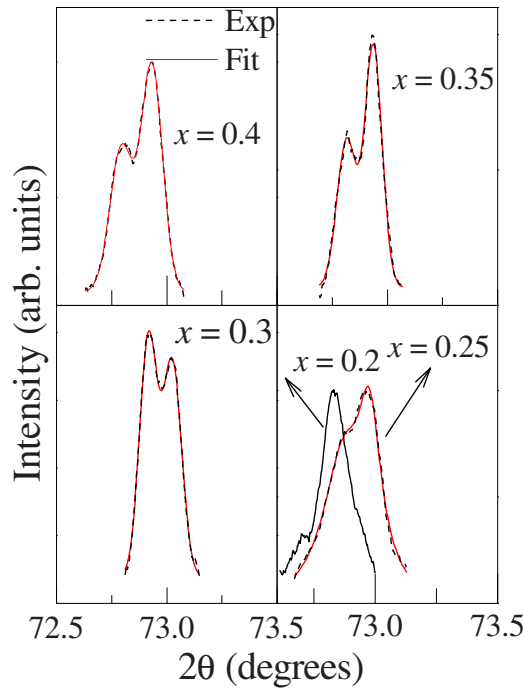


FIG. 4. (Color online) XRD patterns of (440) reflections of $\text{Tb}_x\text{Dy}_{0.9-x}\text{Nd}_{0.1}\text{Fe}_{1.93}$ compounds after fitting.

down below its Curie temperature.^{9,14} On the other hand, a rhombohedral or tetrahedral distortion led by magnetostriction coefficient can be identified. XRD at a slow rate (angle 2θ : 72.5° – 73.5° , step width of 0.002 and time per step of 60 s) was taken on $\text{Tb}_x\text{Dy}_{0.9-x}\text{Nd}_{0.1}\text{Fe}_{1.93}$ to detect the crystal structure distortion. The profiles of the (440) line after eliminating the effect of $\text{K}\alpha_2$ radiation are represented in Fig. 4. When $0.2 > x \geq 0.4$, splitting of the (440) peak into two is clearly observed, indicating that the EMD of these materials is along $\langle 111 \rangle$, indicating a large rhombohedral distortion. The rhombohedral distortion disappeared when $x=0.2$, suggesting that the EMD lies along $\langle 100 \rangle$. Evidently, the tetragonal distortion, which originated from magnetostriction ($\lambda_{100} \sim 0$), is too small to be observed through XRD. The spontaneous magnetostriction is calculated using the equation⁹

$$\lambda_{111} = 2 \frac{d_{440} - d_{\bar{4}\bar{4}0}}{d_{440} + d_{\bar{4}\bar{4}0}},$$

where d_{440} and $d_{\bar{4}\bar{4}0}$ denote the crystallographic plane distances in pseudocubic indices (hkl) and these values are calculated precisely by fitting the experimental data (Fig. 4). The composition dependence of the spontaneous magnetostriction (λ_{111}) is shown in Fig. 5(a). It can be seen from the figure that λ_{111} increases with increasing Tb content in these compounds, in accordance with the observation that TbFe_2 has a larger λ_{111} than DyFe_2 .^{1,5} The maximum λ_{111} is observed for the compound $\text{Tb}_{0.4}\text{Dy}_{0.5}\text{Nd}_{0.1}\text{Fe}_{1.93}$ (1670×10^{-6}) and this compound is near to anisotropy compensation point, and should have small anisotropy similar to

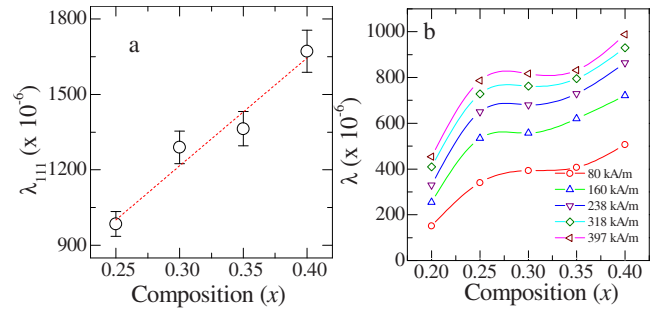


FIG. 5. (Color online) (a) Concentration dependence of the spontaneous magnetostriction (λ_{111}) of the $\text{Tb}_x\text{Dy}_{0.9-x}\text{Nd}_{0.1}\text{Fe}_{1.93}$ compounds. (b) Concentration dependence of the magnetostriction ($\lambda = \lambda_{||} - \lambda_{\perp}$) at room temperature for the polycrystalline $\text{Tb}_x\text{Dy}_{0.9-x}\text{Nd}_{0.1}\text{Fe}_{1.93}$ compounds.

$\text{Tb}_{0.3}\text{Dy}_{0.7}\text{Fe}_{1.93}$. Moreover, in the present investigation, the compound $\text{Tb}_{0.4}\text{Dy}_{0.5}\text{Nd}_{0.1}\text{Fe}_{1.93}$ possesses large parallel magnetostriction value of 1300×10^{-6} (at 5 kOe) and it is larger than that of $\text{Tb}_{0.27}\text{Dy}_{0.73}\text{Fe}_{1.93}$ compound. The composition dependence of magnetostriction ($\lambda = \lambda_{||} - \lambda_{\perp}$) at different magnetic fields for $\text{Tb}_x\text{Dy}_{0.9-x}\text{Nd}_{0.1}\text{Fe}_{1.93}$ compounds is shown in Fig. 5(b). It is clear from the figure that the magnetostriction near $x=0.25$ shows a peak at the low applied magnetic fields, implying low anisotropy due to anisotropy compensation. This observation is consistent with the magnetization data and XRD on magnetically aligned powders.

The results of magnetization, XRD on magnetically aligned samples, and magnetostriction indicate that the anisotropy compensation is near $x=0.25$. The compound $\text{Tb}_{0.4}\text{Dy}_{0.5}\text{Nd}_{0.1}\text{Fe}_{1.93}$ shows larger spontaneous magnetostriction (1670×10^{-6}) and field induced magnetostriction (1300×10^{-6} at 5 kOe), and hence it can be a potential candidate for the practical applications.

One of the authors (S.N.J.) would like to thank Indian Institute of Technology Madras for the financial support.

¹A. E. Clark, in *Ferromagnetic Materials*, edited by E. P. Wohlfarth (North-Holland, Amsterdam, 1980), p. 531.

²N. C. Koon, C. M. Williams, and B. N. Das, *J. Magn. Magn. Mater.* **100**, 173 (1991).

³E. Callen, *Proceedings of the Metallic Magnetoacoustic Materials Workshop*, Boston, edited by F. S. Garter (Office of Naval Research, Arlington, VA, 1969).

⁴N. C. Koon, A. Schindler, and F. Carter, *Phys. Lett. A* **37**, 423 (1971).

⁵A. E. Clark, H. Belson, and N. Tamagawa, *Phys. Lett. A* **42**, 160 (1972).

⁶V. Hari Babu, G. Markandeyulu, and A. Subrahmanyam, *Appl. Phys. Lett.* **90**, 252513 (2007).

⁷W. J. Ren, J. J. Liu, D. Li, W. Liu, X. G. Zhao, and Z. D. Zhang, *Appl. Phys. Lett.* **89**, 122506 (2006).

⁸S. N. Jammalamadaka, G. Markandeyulu, and K. Balasubramaniam, *Appl. Phys. Lett.* **92**, 044102 (2008).

⁹W. J. Ren, Z. D. Zhang, X. G. Zhao, W. Liu, and D. Y. Geng, *Appl. Phys. Lett.* **84**, 562 (2004).

¹⁰C. M. Williams and N. C. Koon, *Physica B* **86–88**, 147 (1977).

¹¹C. Mayer, F. Hartmann–Boutron, Y. Gros, and Y. Berthier, *J. Phys. (France)* **42**, 605 (1981).

¹²Y. G. Shi, S. L. Tang, Y. J. Huang, L. Y. Lv, and Y. W. Du, *Appl. Phys. Lett.* **90**, 142515 (2007).

¹³U. Atzmony and M. P. Dariel, *Phys. Rev. B* **13**, 4006 (1976).

¹⁴A. V. Andreyev, A. V. Deryagin, S. M. Zadvorkin, and V. N. Moskalev, *Phys. Met. Metallogr.* **51**, 64 (1981).

Applied Physics Letters is copyrighted by the American Institute of Physics (AIP). Redistribution of journal material is subject to the AIP online journal license and/or AIP copyright. For more information, see <http://ojps.aip.org/aplo/aplcr.jsp>